LOW LOSS AND HIGH GRADIENT SC CAVITIES WITH DIFFERENT WALL SLOPE ANGLES*

Valery Shemelin

Laboratory for Elementary-Particle Physics, Cornell University, Ithaca, NY 14853

Abstract

The introduction of reentrant shape for superconducting cavities has made it possible to achieve record-high gradients. In this paper it is shown that lowest losses in the cavities are also achievable employing the reentrant shape. Influence of the cavity wall slope angle on the extreme gradient and losses is analyzed.

INTRODUCTION

The reentrant shape was obtained as the best shape for maximal accelerating gradient if we believe that maximal gradient is limited by peak magnetic field and we minimize the value of H_{pk}/E_{acc} for a given overvoltage E_{pk}/E_{acc} on the iris [1]. High gradient tests confirmed this underlying idea and world-record-high CW accelerating gradients of 53 MV/m for 70 mm and 58 MV/m for 60 mm aperture single cell cavities were achieved [2 - 4] at 1300 MHz.

The consecutive usage of optimization algorithm for minimal losses also leads to a reentrant shape of the cavity cell [5]. It was shown [6] that optimization for $G \cdot R/Q$ leads to nearly the same geometry as optimization for H_{pk}/E_{acc}, with difference in these parameters less than 0.2 % at least in the examples presented in that paper. Here, E_{pk}/E_{acc} and H_{pk}/E_{acc} denote ratios of the peak electric and magnetic field on the cell surface to the accelerating gradient in this cell. $G \cdot R/Q$ is the product of the geometry factor and the geometric shunt impedance. This value is a measure of losses in the cavity. For a given surface resistance, losses are inversely proportional to it. Calculations in abovementioned cases were done without limitations of the angle α, Fig. 1, the wall of the cell has relative to the axis of rotation. This freedom has led us in the process of optimization to angles $\alpha < 90^{\circ}$ *i. e.* to reentrant shapes.

However, the reentrant shape is yet not so widely used for superconducting cavities. This is why it is interesting to investigate the dependence of the cavity parameters on this angle. We could judge whether it is worth to overcome some technological challenges attributed to the reentrant shape for the purpose of higher achievable gradient and lower losses. To have this possibility we need to compare cells with limited angle optimized with the same approach as was done without angle limitations and led to reentrant shapes.

THE GEOMETRY FOR OPTIMIZATION

We employ the construction of the cell profile line as two elliptic arcs with half-axes A, B, a, and b, separated by a straight segment of length l, Fig. 1, conjugated to arcs. We talk about a non-reentrant shape if the angle α is more than 90°, Fig. 1a. The reentrant cell can also have a straight segment (Fig. 1b). In earlier optimization [1, 7] the length of this segment appeared to be 0 (Fig. 1c) after consecutive steps of optimization.
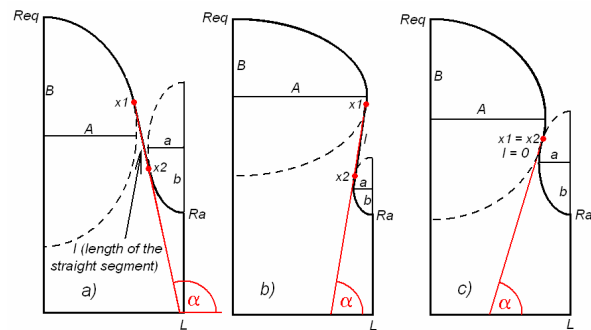

Figure 1: Geometry for optimization.

The radius of the iris aperture Ra is chosen by some additional considerations; it is not the task of this optimization and should be taken as an independent parameter. The length L of the half-cell is taken as a quarter of the wave-length, and boundary conditions correspond to the π-mode. The value of the equatorial radius Req is used for tuning to the working frequency. Sure, a more intricate profile line can give a better eventual result, and we used earlier a description of the profile with 6 circular arcs [7]. However, an improvement of H_{pk}/E_{acc} was not more than 1 % in the case of 6 circle arcs in comparison to 2 elliptic arcs though this optimization can be incomplete because of its complexity.

Adoption of an elliptic arc for the equatorial area is crucial. The problem of cavity electric strength made to take the iris edge in a shape of ellipse far ago. We apply an ellipse to the inductive part of the cell because now we have a problem of magnetic strength.

In optimization with 2 elliptic arcs we have 3 independent parameters for optimization: 3 half-axes (A, B, and a), the fourth one (b) is defined by geometrical restrictions.

If we introduce the limiting angle of slope we need to search the minimum (of H_{pk}/E_{acc} or losses) in a 4-D space: A, B, a, and b under two limiting conditions: E_{pk}/E_{acc} and the angle α are less than definite values.

As a result of these conditions the value of l can be not a zero anymore.

Calculations were done with TunedCell code that is a wrapper code for SLANS and was developed specially for fast optimization [8]. The SLANS code [9] is known as a code with high accuracy [10] that is necessary for our goal.

RESULTS OF OPTIMIZATION

Results of optimization for minimal magnetic peak field are presented in Fig. 2 (solid lines). For easier comparison with the well-known TESLA cavity [11], with $\alpha = 103.2°$, which is a prototype for the ILC, the values of H_{pk}/E_{acc} on the graph are normalized to corresponding values of TESLA (42 Oe/(MV/m)) so that $h = H_{pk}/42E_{acc}$ is equal to 1 for TESLA cells. (According to our calculation, the normalized magnetic peak field appeared about 1 % less than this value, as shown on the graph). Another defining parameter, E_{pk}/E_{acc} which is close to 2 for the TESLA cells, was kept for the upper curve and increased for the next ones. (Again, our calculations give for the TESLA regular cells $E_{pk}/E_{acc} = 1.99$. This is why this point slightly falls out of the curve). 10 % higher electric peak field decreases the magnetic peak field by 7 % as can be seen from the end point of the second solid curve. Sacrifice of next 10 % in electric field decreases h more only by 2 % [1] giving in sum -9 % in h for +20 % in E_{pk}/E_{acc}. The aperture radius $Ra = 35$ mm for the first group of curves is the same as in TESLA inner cells while it is 30 mm for another group. Influence and possible benefit for higher gradient from decreasing the aperture is much higher than from increasing the overvoltage E_{pk}/E_{acc}. Smaller aperture causes smaller coupling and hence worst field flatness, also as higher wake fields. However it is shown that ILC will tolerate the cavities with the new (reentrant) shape and the smaller iris diameter [12].

Results of optimization for maximal $G \cdot R/Q$ are presented in Fig. 3. They are also normalized for the TESLA value: $g \cdot r/q = (G \cdot R/Q)/(30800 \text{ Ohm}^2)$.

The extreme left points of curves in Figs 2 and 3 correspond to minimal length of the straight segment: $l = 0$ when the cell presents two conjugated elliptic arcs, the geometry discussed earlier [1, 6, 7].

When optimizing for max $G \cdot R/Q$, the values of h slightly increase, these dependences are shown in Fig. 2 by dash lines. When we optimize for min h, values of $G \cdot R/Q$ become somehow smaller than immediately by maximization of $G \cdot R/Q$. There is an attempt to show this in Fig. 3 by dashed lines but actually these lines graphically coincide with the solid ones. This means that we don't need to optimize for max $G \cdot R/Q$ - optimization for min h gives us the shapes that have

practically minimal losses! When we try to optimize for max $G \cdot R/Q$, maximal magnetic field shifts to smaller radius because the losses depend not only on the value of the field but also on the value of area where it exists. Smaller radii can give smaller contribution to losses even if they have higher field. However, this change is negligible if we optimize for max $G \cdot R/Q$. Minimal peak magnetic field secures low losses in the whole cavity.
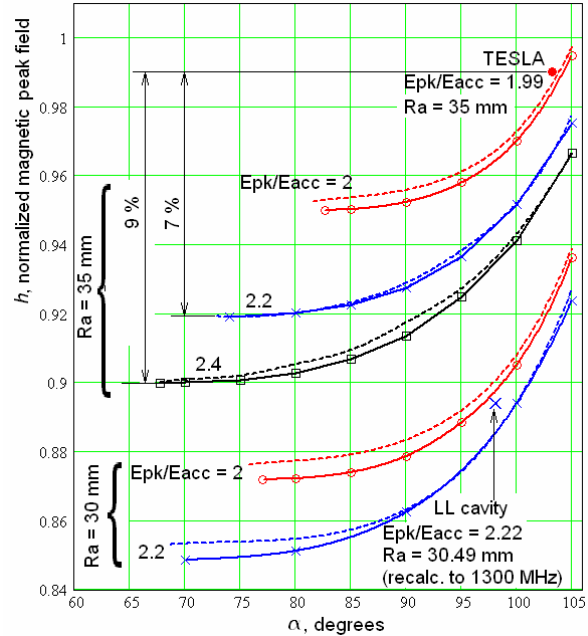

Figure 2: Normalized magnetic peak field for different angles of slope. Solid lines present optimization for min h, dash lines are for max $G \cdot R/Q$.
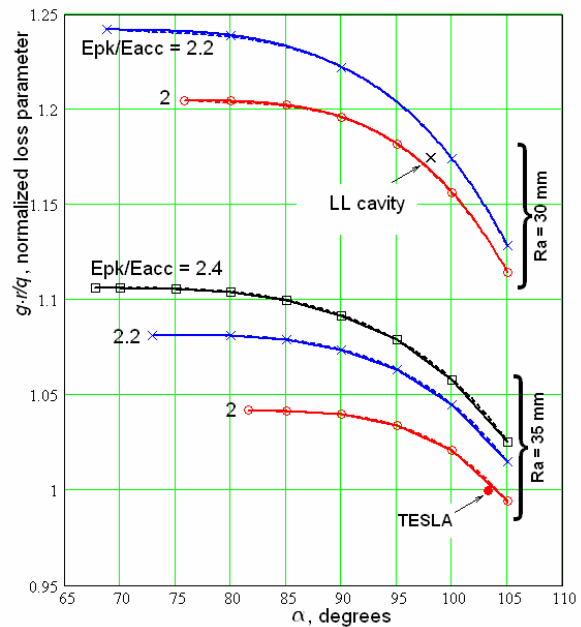

Figure 3: Normalized loss parameter for different angles of slope. Solid lines are for max $G \cdot R/Q$, dash lines are for minimal h. (Graphically both lines nearly overlap).

07 Accelerator Technology Main Systems

T07 Superconducting RF

Distributions of the magnetic field along the profile line of the cells with $Ra = 30$ mm, $E_{pk}/E_{acc} = 2.2$ and with minimal slope angle (lowest curves in Fig. 2 and the uppers in Fig. 3, extreme left points with $l = 0$) for both cases of optimization are shown in Fig. 4.
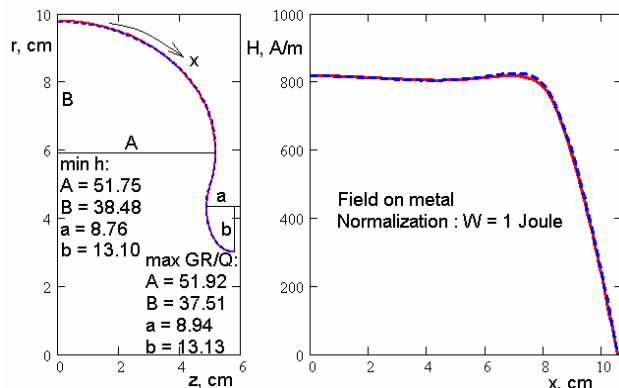

Figure 4: Geometries of the cells (left picture) with min h (red solid line) and max $G \cdot R/Q$ (blue dashed line) practically coincide. Difference in magnetic fields along the profile lines of the cell (right) is also negligible. *A, B, a* and *b* are half-axes of elliptic arcs.

There is also shown on the graphs of Fig. 2 and 3, the cell of the low-loss (LL) cavity of JLab [13]. This well-optimized geometry takes its place on our graphs corresponding to its aperture and slope angle (98.0°). Its position on the graphs is defined also by $E_{pk}/E_{acc} = 2.22$ and $Ra = 30.49$ mm (recalculated to 1300 MHz). These examples, both TESLA and LL, show that cavity cells can be compared only taking into account their E_{pk}/E_{acc} ratio, aperture radius Ra and the wall slope angle. After the choice of these values, the correct optimization should be done, and other figures of merit can be obtained. And there is no necessity to optimize for low losses because optimization for lowest peak magnetic field successfully serves to both goals: highest gradients and lowest losses.

Calculation of elliptic arc parameters, namely *A, B, a,* and *b,* for both cases of optimization, appeared a time-consuming task not only because of 4-dimensional space of these parameters but also because of a very small change of h in some cases when this parameters are varied. Gradients of the functions could not be calculated because the computational noise becomes higher than accuracy of calculations for small steps. To avoid false local minima the dependences of these parameters on α were also analyzed. First results of these calculations gave smooth curves $h(\alpha)$ but points for dependences $A(\alpha), B(\alpha)$ and so on were scattered. After more accurate calculation most points fell on smooth curves though corrections of $h(\alpha)$ were mainly in the fourth digit. Results for these dependences and other details will be presented in our inner report [14].

CONCLUSION

Dependences of the normalized magnetic peak field H_{pk}/E_{acc} and the loss parameter $G \cdot R/Q$ on the wall slope angle of elliptic shape cavities are analyzed. It is shown that optimization for minimal magnetic peak field secures also low losses in the cavity with any slope angles. Increasing the normalized electric field E_{pk}/E_{acc}, decreasing the aperture, and exploiting the reentrant shapes (slope angle $\alpha < 90°$) the record-high gradients and record-low losses can be achieved.

ACKNOWLEDGMENT

The author is thankful to Hasan Padamsee for helpful discussion and advice.

REFERENCES

[1] V. Shemelin, H. Padamsee, R. L. Geng, "Optimal cells for TESLA accelerating structure," Nucl. Instr. and Meth. A 496, 1 (2003).

[2] R. L. Geng, H. Padamsee, A. Seaman, V. D. Shemelin, "World record accelerating gradient achieved in a superconducting niobium RF cavity," PAC 2005, p. 653-655.

[3] R. L Geng, H. Padamsee, V. Shemelin, "High gradient studies for ILC with single cell re-entrant shape and elliptical shape cavities made of fine-grain and large-grain niobium," this conference.

[4] F. Furuta, K. Saito, et al., "Experimental comparison at KEK of high gradient performance of different single cell superconducting cavity designs," EPAC 2006, pp. 750-752.

[5] S. Belomestnykh, V. Shemelin, "High-β cavity design," 12th Int. Workshop on RF superconductivity, Ithaca, NY, USA, July 10-15, 2005.

[6] V. Shemelin, "Reentrant cavities have highest gradient and minimal losses simultaneously," Cornell University LEPP Report SRF 051010-09, 2005.

[7] V. Shemelin, H. Padamsee, "The optimal shape of cells of a superconducting accelerating section," Cornell University LNS Report SRF 0201128-01, 2002; TESLA Report 2002-1.

[8] Dmitry Myakishev, "TunedCell," Cornell University LEPP Report SRF/D 051007-01.

[9] D. G. Myakishev, V. P. Yakovlev, "The new possibilities of SuperLANS code for evaluation of axisymmetric cavities," PAC1995, May 1-5, 1995, Dallas, Texas, pp. 2348-2350.

[10] S. Belomestnykh, "Spherical cavity: Analytical formulas. Comparison of computer codes," Cornell University LNS Report SRF 941208-13. 1994.

[11] B. Aune et al., "Superconducting TESLA cavities," Phys. Rev. ST-Accel. Beams 3, 092001 (2000).

[12] Igor Zagorodnov, Nikolay Solyak, "Wakefield effects on new ILC cavity shapes," EPAC 2006, Edinburgh, Scotland, pp. 2862-2864.

[13] J. Sekutovicz et al., "Cavities for JLab's 12 GeV upgrade," PAC 2003, p. 1395-1397.

[14] V. Shemelin. "High gradient and low loss SC cavities with different wall slope angles," Cornell University LEPP report SRF 070614-02, 2007.